

# On the Determination of the Rotational Oblateness of Achernar

A. C. Carciofi<sup>1</sup>, A. Domiciano de Souza<sup>2</sup>, A. M. Magalhães<sup>1</sup>, J. E. Bjorkman<sup>3</sup>, F. Vakili<sup>2</sup>

## ABSTRACT

The recent interferometric study of Achernar, leading to the conclusion that its geometrical oblateness cannot be explained in the Roche approximation, has stirred substantial interest in the community, in view of its potential impact in many fields of stellar astrophysics. It is the purpose of this paper to reinterpret the interferometric observations with a fast rotating, gravity darkened central star surrounded by a small equatorial disk, whose presence is consistent with contemporaneous spectroscopic data. We find that we can only fit the available data assuming a critically rotating central star. We identified two different disk models that simultaneously fit the spectroscopic, polarimetric, and interferometric observational constraints: a tenuous disk in hydrostatic equilibrium (i.e., with small scaleheight) and a smaller, scaleheight enhanced disk. We believe that these relatively small disks correspond to the transition region between the photosphere and the circumstellar environment, and that they are probably perturbed by some photospheric mechanism. The study of this interface between photosphere and circumstellar disk for near-critical rotators is crucial to our understanding of the Be phenomenon, and the mass and angular momentum loss of stars in general. This work shows that it is nowadays possible to directly study this transition region from simultaneous multi-technique observations.

*Subject headings:* polarization — interferometry — spectroscopy — stars: emission line, Be — stars: individual (Achernar)

---

<sup>1</sup>Instituto de Astronomia, Geofísica e Ciências Atmosféricas, Universidade de São Paulo, Rua do Matão 1226, Cidade Universitária, São Paulo, SP 05508-900, Brazil

<sup>2</sup>LUAN, Université de Nice-Sophia Antipolis (UNSA), CNRS, Observatoire de la Côte d’Azur (OCA), 28 avenue de Valrose, Parc Valrose, F-06108 Nice - France

<sup>3</sup>University of Toledo, Department of Physics & Astronomy, MS111 2801 W. Bancroft Street Toledo, OH 43606 USA

## 1. Introduction

Interferometry greatly increased our knowledge of the Be Star Achernar ( $\alpha$  Eri, HD10144). Domiciano de Souza et al. (2003, hereafter D03) observed Achernar during fall 2002 with the ESO-VLTI/VINCI instrument (Kervella et al. 2003) in the  $K$  band and found that the star is highly oblate. By converting the individual visibilities into equivalent uniform disk angular diameters they derived a ratio between the maximum and minor elongation axis  $a/b = 1.56 \pm 0.05$ . Later, Kervella & Domiciano de Souza (2006) detected a tenuous polar wind and very recently Kervella & Domiciano de Souza (2007) found that Achernar has a main-sequence, lower mass companion.

The available interferometric data, together with the abundance of data from the literature, forms a body of information that is probably unrivaled by that of any other Be star. There is, however, much that is still unknown about the star and its circumstellar environment. As pointed out by D03, the determination of the actual stellar oblateness from the interferometric data is not a simple task, since there are so many unknowns involved. In their original work D03, based on simultaneous spectroscopic data, assumed that there was no circumstellar material at the time of the observations, and that the observed shape was purely photospheric in origin. Their modeling of the observations with a rotationally deformed, gravity darkened star, assuming the Roche approximation of uniform rotation and centrally condensed mass, led to the conclusion that the stellar flattening required to explain the observations exceeds that of a critical rigid rotator .

Recent theoretical developments in the theory of differentially rotating stars (e.g., Jackson et al. 2004) show that they can have equatorial radii larger than the Roche limit, which is physically compatible with the interferometric results. However, Vinicius et al. (2006) demonstrated the existence of a tiny, yet non negligible emission in  $H\alpha$  at the time of the VLTI observations, an indication that there was some circumstellar material around Achernar, probably associated with a small rotating disk. Furthermore, Vinicius et al. (2006) showed, from temporal analysis of profile variations of the line He I  $\lambda 6678$  Å, that orbiting gas clouds are a very frequent feature of Achernar, even during its quiescent phase.

The presence of this circumstellar material raises the question of how much it can contribute to the observed visibilities. In this paper we investigate how the presence of a small disk around Achernar may alter to the interferometric signal, and the effects this may have on determination of fundamental parameters such as stellar rotation rate and stellar flattening.

## 2. Models

To compute the emergent spectrum of the system we use the computer code HDUST (Carciofi & Bjorkman 2006; Carciofi et al. 2006). This code solves the coupled problem of the non-local thermodynamic equilibrium (NLTE) and radiative equilibrium for arbitrary three-dimensional envelope geometries, using the Monte Carlo method. Given a prescription for the star (rotation rate, shape, flux distribution, effective temperature, luminosity, etc.) and for the circumstellar gas (density and velocity distribution) the code calculates the NLTE Hydrogen level populations and the electron kinetic temperature. Once those quantities are determined, the emergent spectrum (spectral energy distribution, line profiles, polarization, synthetic images, etc.) is calculated.

For the present work, we modified HDUST to treat non-spherical, gravity darkened stars. We assume the stellar shape to be an spheroid, which is a reasonable approximation for the shape of a rigidly rotating star (Frémat et al. 2005). Given the stellar rotation rate,  $\Omega/\Omega_{\text{crit}}$ , the ratio between the equatorial and polar radii is determined from the Roche approximation for the stellar surface equipotentials (Frémat et al. 2005). For the gravity darkening we use the standard von Zeipel flux distribution (von Zeipel 1924), according to which  $F(\theta) \propto g_{\text{eff}}(\theta) \propto T_{\text{eff}}^4(\theta)$ , where  $g_{\text{eff}}$  and  $T_{\text{eff}}$  are the effective gravity and temperature at stellar latitude  $\theta$ . In HDUST, the star is divided into a number of latitude bins (typically 50) which have an associated  $T_{\text{eff}}$  and  $g_{\text{eff}}$  and emit with an spectral shape given by the corresponding Kurucz model atmosphere (Kurucz 1994).

For the disk density distribution we assume the following expression

$$\rho(\varpi, z) = \frac{\rho_0 R_{\text{eq}}}{\sqrt{2\pi}H} \left( \frac{R_{\text{eq}}}{\varpi} \right)^2 \exp(-z^2/H^2), \quad (1)$$

which is similar to the density distribution of an isothermal viscous decretion disk in vertical hydrostatic equilibrium (e.g. Carciofi et al. 2006). In the above equation,  $\varpi$  is the radial distance in cylindrical coordinates,  $R_{\text{eq}}$  is the equatorial radius of the star and  $\rho_0$  is the disk density scale. We write the disk vertical scaleheight,  $H$ , as

$$H = H_0 (\varpi/R_{\text{eq}})^{1.5}, \quad (2)$$

where  $H_0$  is the scaleheight at the base of the disk. For isothermal disks in vertical hydrostatic equilibrium  $H_0 = aV_{\text{crit}}^{-1}R_{\text{eq}}$ , where  $a$  is the sound speed and the critical velocity,  $V_{\text{crit}} \equiv (GM/R_{\text{eq}})^{1/2}$ , is the Keplerian orbital speed at the stellar surface.

We chose a set of fixed stellar parameters, listed in Table 1. The value for the polar radius came directly from the interferometry, once we fixed the stellar inclination angle to

be 65 deg after the recent work of Carciofi et al. (2007). It is worthy noting, however, that the results we show below are little affected if we allow the inclination angle to vary within a reasonable range (say,  $\pm 5$  deg). The value for the stellar luminosity was obtained by fitting the available photometric data (see caption of Figure 1).

Each model of the star plus disk system has 4 free parameters: (1) the stellar angular rotation rate,  $\Omega/\Omega_{\text{crit}}$ , (2) the disk density scale,  $\rho_0$ , (3) the disk outer radius,  $R_d$ , and (4) the disk scaleheight,  $H_0$ .

We have two well-known observational constraints, viz., the 2002 interferometric observations (D03) and the 2002 H $\alpha$  line profile (Vinicius et al. 2006, fig. 12). Unfortunately, no contemporaneous measurement of the linear polarization exists, but we can impose, with a reasonable level of confidence, an upper limit for the polarization based on the recent results of Carciofi et al. (2007). In that paper, the results of a polarization monitoring of Achernar, carried out between 2006 July and November, is reported. Those measurements were taken during a period in which Achernar was active, with a tenuous circumstellar disk, as indicated by the weak H $\alpha$  emission (Carciofi et al. 2007, fig. 3). We adopt as an upper limit for the polarization in our modeling the lowest value reported in Carciofi et al. (2007), which was 0.12% in the  $B$  band. As we shall see below, fixing this upper limit for the polarization level has important consequences for the modeling.

### 3. Results

Our modeling procedure is as follows. For a given set of  $\Omega/\Omega_{\text{crit}}$ ,  $\rho_0$ ,  $R_d$  and  $H_0$  we calculate synthetic images in the  $K$  band, centered at  $\lambda = 2.15 \mu\text{m}$ , the H $\alpha$  line profile, the continuum polarization and the spectral energy distribution (SED). The model amplitude visibilities were obtained from the Fourier transform moduli of the model images at  $2.15 \mu\text{m}$ , normalized by the total  $K$  band flux of the synthetic image.

Since the H $\alpha$  emission from October 2002 is very small and the true photospheric profile of Achernar is not known, we model, instead of the observed profile, the residual emission profile of Vinicius et al. (2006), fig. 12. This profile was obtained by subtracting from the October 2002 observations the average profile of the 1999 period, which is believed to be purely photospheric. The equivalent width (hereafter EW) of this emission profile is  $-0.29 \text{ \AA}$ .

In Figure 2 we show the visibility curves along the polar and equatorial directions together with the corresponding  $K$  band images for five representative models that were chosen to illustrate different aspects of our solution. In Table 2 we list the model parameters,

along with some model results, such as the  $B$  band polarization level, the  $H\alpha$  EW and the  $K$  band flux excess,  $E_K$ , which is defined as  $F^\lambda/F_\star^\lambda - 1$ , where  $F_\star^\lambda$  is the stellar flux without the disk at wavelength  $\lambda$ .

Let us begin discussing models 1 to 3, for which the star was assumed to be rotating critically. We have used  $\Omega/\Omega_{\text{crit}} = 0.999999$  ( $V_{\text{eq}}/V_{\text{crit}} = 0.9993$ ) instead of 1 to avoid the unphysical situation of having  $T_{\text{eff}} = 0$  in the stellar equator. Model 1 corresponds to a small and relatively dense disk, with  $H_0$  given by Eq. 2, i.e., model 1 corresponds to a disk in vertical hydrostatic equilibrium. For this model the visibility curves matches very well the observations and the polarization is within the adopted limit, but the  $H\alpha$  emission is very weak, as a result of the small disk size.

One way to increase the  $H\alpha$  emission is to make the disk larger. For model 2 we adopted a larger value for  $R_d$ , but the density had to be decreased in order to keep the polarization within the adopted limit. This model reproduces well both the visibility curves and the  $H\alpha$  EW.

Another way of increasing the line emission is to raise the disk scaleheight. If one raises  $H$  by a factor of, say,  $k$ , the disk density scale must be decreased by a factor  $k^{1/2}$  to keep the polarization approximately constant. Model 3 corresponds to our best scaleheight enhanced model for a critically rotating star. The visibility curves and the  $H\alpha$  EW are well reproduced by the model, and the polarization is within the adopted upper limit.

We also studied models with lower values of  $\Omega/\Omega_{\text{crit}}$ . In this case, our attempts to fit simultaneously the visibility curves, polarization and  $H\alpha$  EW were unsuccessful.

Models 4 and 5 are examples of the results we have obtained for sub-critical stars. Model 4 corresponds to a small and dense disk in vertical hydrostatic equilibrium. This model reproduces quite well the visibilities, but have too large  $B$  band polarization and no  $H\alpha$  emission. A scaleheight enhanced model with lower density, such as model 5, have better values for polarization and  $H\alpha$  EW, but does not have enough IR flux in the equator to account for the observed size.

Our lack of success on fitting the observations with sub-critical models is a direct result of two physical effects, both related to the presence of gravity darkening. For the critical models 1 to 3, the bolometric stellar flux at the equator is about 1100 times lower than the flux at the pole. Since the disks are relatively small and the star oblate, light from the pole cannot reach the disk and, as a result, the net scattered flux is small. As  $\Omega/\Omega_{\text{crit}}$  decreases, the flux at the equator rises, and the star becomes less oblate. Both mechanisms cause a significant increase in the scattered flux and, thus, in the polarization level.

## 4. Discussion

The presence of a small disk around Achernar is a realistic possibility to explain the interferometric observations. As shown by D03 (see also Figure 1), Roche models without a disk cannot account for the observed aspect ratio.

The combined constraints imposed by the interferometry, spectroscopy and the adopted upper limit for the polarization have allowed us to impose very narrow limits on the model parameters, within our assumption of a rigidly rotating star in the Roche approximation surrounded by a small disk. The main result is that the star must be rotating very close to critical, since all of our models with  $\Omega/\Omega_{\text{crit}} < 0.992$  that successfully reproduced both the visibilities and the  $H\alpha$  EW (e.g. model 5) had too large polarization levels, for the reasons discussed above.

We have found two critical models that reproduce equally well the observations: a large and dense disk in hydrostatic equilibrium (i.e., geometrically thin; model 2) and a small and more tenuous disk with enhanced scaleheight (i.e., geometrically thick; model 3). Because the lack of contemporaneous polarization measurements, the model parameters shown in Table 2 have a degree of uncertainty that is difficult to estimate. This stresses the importance of having simultaneous multi-technique data.

The current paradigm for Be star disks is that of a geometrically thin viscous Keplerian disk in vertical hydrostatic equilibrium. This paradigm has been corroborated by several recent studies (e.g. Carciofi et al. 2006; Meilland et al. 2007).

When a star is close to critical rotation, the stellar photospheric material near the equator, which is weakly bound to the star because of the strong centrifugal force, can eventually escape the star provided it is given an extra energy by some other mechanism (e.g. stellar pulsation, interaction in a binary system, photospheric activity). This material is likely to have, initially, a very complicated density and velocity distribution. As the gas diffuses outwards as a result of viscosity, the density and velocity distributions will tend to relax and become in hydrostatic equilibrium.

Thus, it is reasonable to assume that there is a *transition region* between the photosphere (which is characterized by large densities of the order of  $10^{-10}$  g cm<sup>3</sup>) and the disk itself, which has densities at least 10 times lower. Many unknowns exist concerning the size and physical properties (e.g. density, temperature, velocity field) of this smooth transition region.

With the available data we were able to narrow down substantially the range of possible values for Achernar’s model parameters, but we cannot distinguish yet between model 2 and 3, i.e., between a model in hydrostatic equilibrium and a model with enhanced scaleheights

that might result from the perturbation of the gas by some photospheric mechanism.

As shown in Figure 1, high-precision spectropolarimetry might add invaluable information, since models 2 and 3 have different values for the size of Balmer and Paschen jumps in polarization. Also, with simultaneous spectro-interferometry and spectropolarimetry one can spatially resolve the velocity field, thus establishing whether the material is in equilibrium or not. The observed residual emission profile (Figure 1) is indicative of velocities fields more complex than the simple Keplerian rotation that was assumed in this work.

In any case, one important consequence of this work is that we have shown that with current observing techniques and state-of-the-art modeling it is already possible to study the properties of the very inner layers of the disk in Achernar and possibly other nearby Be stars. Future simultaneous spectropolarimetry, spectro-interferometry and photometry will allow us to study the properties of this region and determine, for instance, the size of the transition region and the point at which the disk becomes in vertical hydrostatic equilibrium.

This work was supported by FAPESP grant 04/07707-3 to ACC, FAPESP grant 01/12598-1 to AMM and NSF grant AST-0307686 to the University of Toledo (JEB). AMM also acknowledges partial support by CNPq.

## REFERENCES

- Carciofi, A. C., & Bjorkman, J. E. 2006, *ApJ*, 639, 1081
- Carciofi, A. C., Miroshnitchenko, A. S., Kusakin, A. V., et al. 2006, *ApJ*, 652, 1617
- Carciofi, A. C., Magalhães, A. M., Leister, N. V., Bjorkman, J. E., & Levenhagen, R. S. 2007, *ApJ*, in press
- Cutri, R. M., et al. 2003, The IRSA 2MASS All-Sky Point Source Catalog, NASA/IPAC Infrared Science Archive. <http://irsa.ipac.caltech.edu/applications/Gator/>
- Domiciano de Souza, A., Kervella, P., Jankov, S., Abe, L., Vakili, F., di Folco, E., & Paresce, F. 2003, *A&A*, 407, L47 (D03)
- Frémat, Y., Zorec, J., Hubert, A.-M., & Floquet, M. 2005, *A&A*, 440, 305
- Jackson, S., MacGregor, K. B., & Skumanich, A. 2004, *ApJ*, 606, 1196
- Kervella, P., et al. 2003, *Proc. SPIE*, 4838, 858

- Kervella, P., & Domiciano de Souza, A. 2006, *A&A*, 453, 1059
- Kervella, P., & Domiciano de Souza, A. 2007, *A&A*, 474, L49
- Kurucz, R. L. 1994, Kurucz CD-ROM No. 19, 20, 21, Cambridge Mass.: Smithsonian Astrophysical Observatory
- Meilland, A., Stee, P., Vannier, M. et al. 2007, *A&A*, 464, 59
- Perryman, M. A. C., Lindegren, L., Kovalevsky, J., et al. 1997, *A&A*, 323, L49
- Vinicius, M. M. F., Zorec, J., Leister, N. V., & Levenhagen, R. S. 2006, *A&A*, 446, 643
- Zacharias, N., Monet, D. G., Levine, S. E., Urban, S. E., Gaume, R., & Wycoff, G. L. 2005, *VizieR Online Data Catalog*, 1297, 0
- von Zeipel, H. 1924, *MNRAS*, 84, 665



Table 1. Fixed Stellar Parameters.

Parameter	Value	Reference
$R_{\text{pole}}$	$7.3 R_{\odot}$	This work
Luminosity	$3150 L_{\odot}$	This work
$V_{\text{crit}}$	$350 \text{ km s}^{-1}$	Vinicius et al. (2006)
inclination	65 deg	Carciofi et al. (2007)
distance	44.1 pc	Perryman et al. (1997)

Table 2. Model Parameters.

Model	$\Omega/\Omega_{\text{crit}}$	$\rho_0 \text{ (g cm}^{-3}\text{)}$	$R_{\text{d}}$	$H \text{ (} R_{\odot}\text{)}$	$\frac{R_{\text{eq}}}{R_{\text{p}}}$	$\frac{T_{\text{p}}}{T_{\text{eq}}}$	H $\alpha$ EW ( $\text{\AA}$ )	$P_B \text{ (\%)}$	$E_K$
1	0.999999	$1.0 \times 10^{-11}$	13.7	0.45	1.5	5.8	0.10	0.02	0.17
2	0.999999	$3.8 \times 10^{-12}$	19.1	0.45	1.5	5.8	-0.34	0.10	0.14
3	0.999999	$2.6 \times 10^{-12}$	16.1	1.1	1.5	5.8	-0.27	0.12	0.12
4	0.992	$1.0 \times 10^{-11}$	13.7	0.45	1.4	1.8	0.20	0.31	0.15
5	0.992	$1.7 \times 10^{-12}$	13.7	0.91	1.4	1.8	-0.05	0.15	0.03

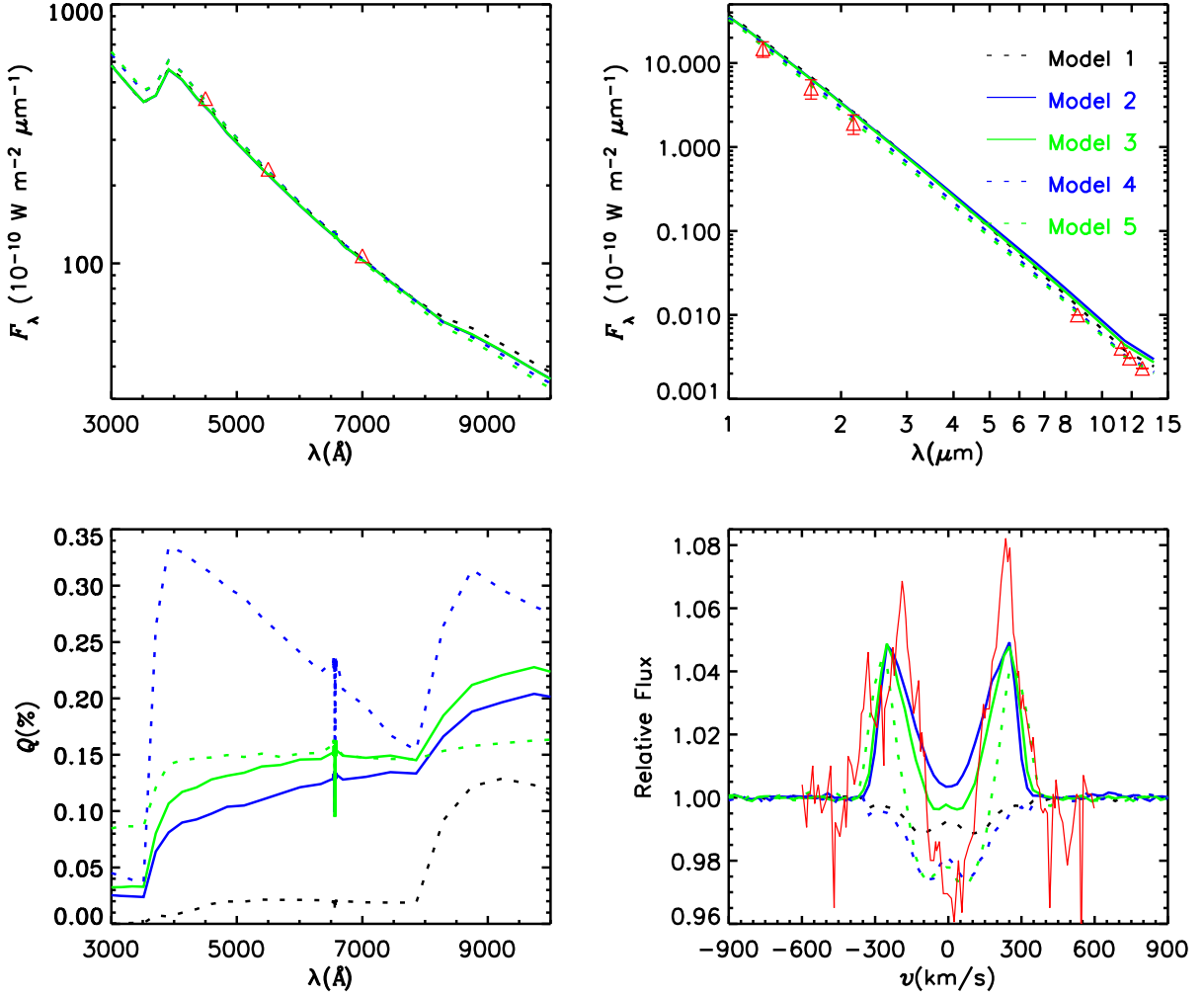


Fig. 1.— Emergent spectrum for models 1 to 5. Top left: visible SED. The red triangles correspond to BVR photometry from the NOMAD catalog (Zacharias et al. 2005), for which no observational errors were available. Top right: IR SED. The JHK photometry is from the 2MASS catalog (Cutri et al. 2003) and the mid-IR photometry is from Kervella & Domiciano de Souza (2007). The observational errors for the mid-IR data is of the order of 2%. Bottom left: continuum polarization. Bottom right: H $\alpha$  emission profile. The red curve corresponds to the residual emission profile of Vinicius et al. (2006).

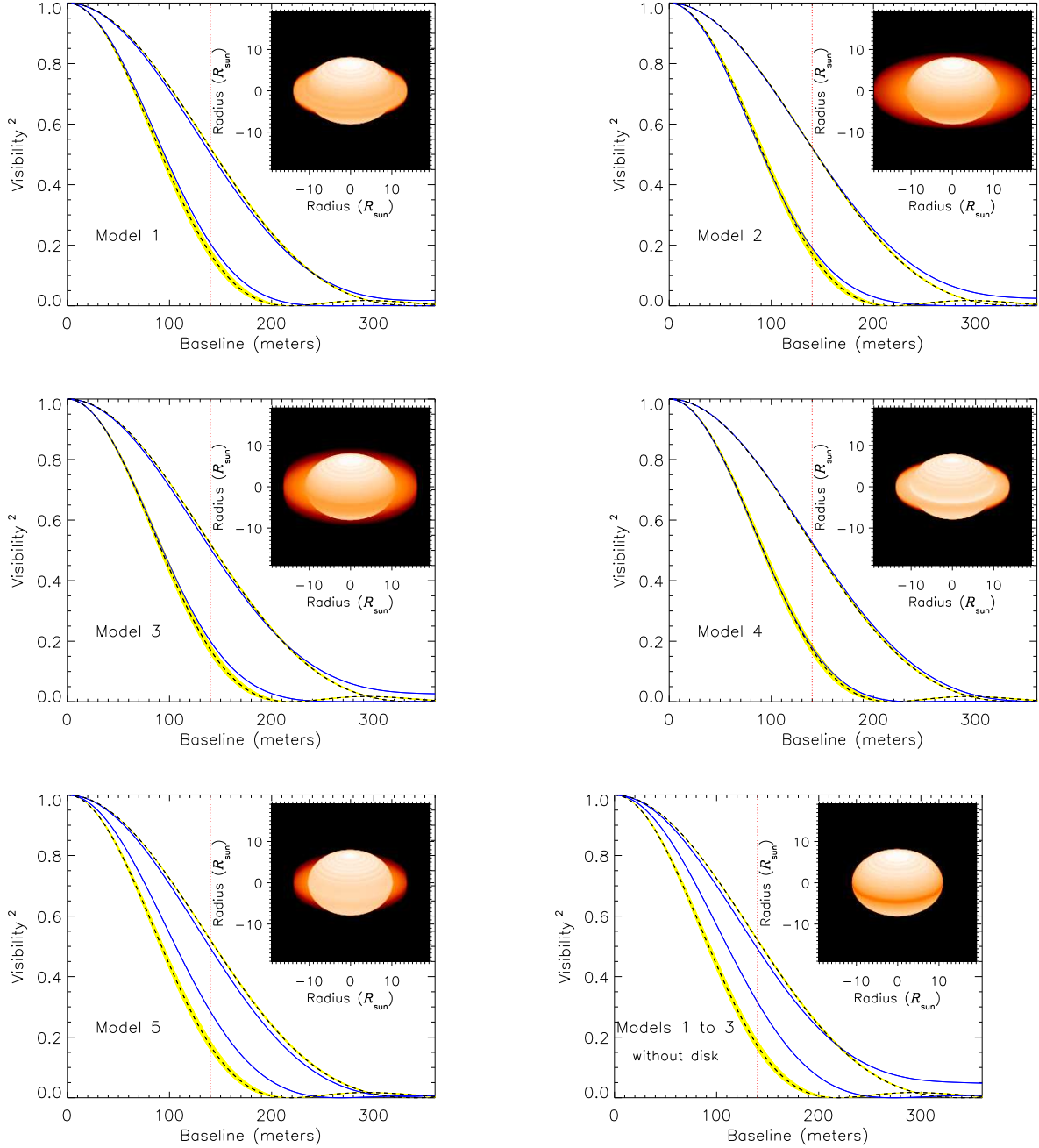


Fig. 2.— Squared visibilities for the models of Table 2 (solid lines), along the polar (upper curves) and equatorial (lower curves) directions. The dashed lines represent the  $K$  band visibilities for uniform disk (UD) angular diameters of 1.62 mas and 2.53 mas derived by D03; the corresponding  $\pm 1$ -sigma uncertainties are shown as light-color bands. These UD diameters indicate the maximum (equatorial direction) and minimum (polar direction) sizes measured on Achernar in the  $K$  band with VLT/IVIC. The vertical dotted lines indicate the maximum baseline available from the VLT/IVIC data. The insets show the model image in the  $K$  band, in logarithmic scale. The bottom right plot shows the squared visibilities for a gravity darkened Roche star at near-critical velocity (models 1 to 3) without the disk, and indicates, as shown by D03, that such model does not reproduce the observations.